Eur Biophys J (2001) 29: 579–586
DOI 10.1007/s002490000115

ARTICLE

**Léa Jaccoud El-Jaick · Daniel Acosta-Avalos
Darci Motta de Souza Esquivel · Eliane Wajnberg
Marilia Paixão Linhares**

Electron paramagnetic resonance study of honeybee *Apis mellifera* abdomens

Received: 25 February 2000 / Revised version: 3 July 2000 / Accepted: 22 August 2000 / Published online: 21 November 2000

Abstract Although ferromagnetic material has been detected in *Apis mellifera* abdomens and identified as suitable for magnetic reception, physical and magnetic properties of these particles are still lacking. Electron paramagnetic resonance is used to study different magnetic materials in these abdomens. At least four iron structures are identified: isolated Fe^{3+} ions, amorphous FeOOH, isolated magnetite nanoparticles of about 3×10^2 nm^3 and 10^3 nm^3 volumes, depending on the hydration degree of the sample, and aggregates of these particles. A low-temperature transition (52–91 K) was observed and the temperature dependence of the magnetic anisotropy constant of those particles was determined. These results imply that biomineralized magnetites are distinct from inorganic particles and the parameters presented are relevant for the refinement of magnetoreception models in honeybees.

Key words Honeybee · Magnetoreception · Electron paramagnetic resonance · Magnetite

Introduction

Living beings are sensitive to environmental signals. Animals orient themselves during migration or homing using sunlight, skylight polarization, stars, winds, geomagnetic field, etc. (Schmidt-Koenig and Keeton 1978; Kirschvink et al. 1985). Animal species differ one from the other in their use of these environmental signals. Magnetoreception, the animal mechanism to detect the geomagnetic field, is still unknown and its origin remains a complex matter (Wiltschko and Wiltschko 1995). Several hypotheses and models have been postulated to explain different mechanisms for different species (Leask 1977; Gould 1985; Kirschvink and Walker 1985; Presti 1985; Rosenblum et al. 1985; Yorke 1985; Sakaki and Motomiya 1990; Edmons 1992; Grissom 1995; Deutschlander et al. 1999; Shcherbakov and Winklhofer 1999). Some of them discuss the nature of the magnetic sensory receptors, suggesting biomineralized magnetic nanoparticles as transducers for the magnetic field information. Lohmann and Johnsen (2000) emphasized that magnetoreceptors have not yet been identified unambiguously in any animal, but it is interesting to point out that, more recently, magnetite has been defined as the magnetoreceptor in rainbow trout (Diebel et al. 2000). Also recently, Lohmann and Johnsen (2000) emphasized that magnetoreceptors have not yet been identified unambiguously in any animal. As the ion oxide magnetite is a common biomineral (Lowenstam 1981), being widely produced in nature from bacteria (Blakemore 1975) to human beings (Kirschvink et al. 1992; Schultheiss-Grassi et al. 1999), it is a good candidate to be the magnetoreceptor.

Insects are certainly the most diversified and populous group of animals. Wiltschko and Wiltschko (1995) and Vácha (1997) have reviewed the influence of the geomagnetic field on the behaviour of a wide variety of insects. Until now, the largest number of behavioural studies related to the geomagnetic field sensitivity were carried out for the honeybee *Apis mellifera* (Wiltschko and Wiltschko 1995). Studies on orientation and navigation tasks of these honeybees reveal the use of the sun compass, the skylight polarization, and the geomagnetic field (Gould 1982). Based on the ferromagnetic hypothesis for magnetoreception (Kirschvink 1989), which

L.J. El-Jaick (✉) · D. Acosta-Avalos[1]
D. Motta de Souza Esquivel · E. Wajnberg
Centro Brasileiro de Pesquisas Físicas,
Rua Dr. Xavier Sigaud 150, CEP 22290,
180 Rio de Janeiro, Brazil
E-mail: leajj@cbpf.br

M. Paixão Linhares
Instituto de Física, Universidade Federal do Rio de Janeiro,
Ilha do Fundão, Rio de Janeiro, Brazil

Present address:
[1]Instituto de Física,
Pontifícia Universidade Católica,
Rua Marquês de São Vicente 225,
CEP 22453, 900 Rio de Janeiro, Brazil

assumes that magnetic particles are involved in magnetoreception, studies of the magnetic properties of the whole honeybee body have shown the presence of magnetite nanoparticles, characterized by its Curie temperature (Gould et al. 1978). Supposing 100 nm nanoparticle diameters, the magnetization measured is in good agreement with 15×10^6 single domains of magnetite nanoparticles found in the front third of the abdomen and aligned transversely to the body axis on their horizontal plane. Later studies on demagnetized bees estimated 2×10^8 superparamagnetic particles of magnetite within the 30–35 nm size range (Gould et al. 1980). Different experiments aimed at the localization of sensory magnetic particles in honeybees have been performed and are reviewed in Vácha (1997). Electron microscopy results from magnetic extracts of worker honeybee abdomens (Kirschvink et al. 1993) evidenced two fractions of magnetite nanoparticles: one 15–30 nm in diameter and another with 3–5 nm diameter. These magnetite nanoparticles were only analysed by magnetization measurements.

Electron paramagnetic resonance (EPR) has proved to be a useful technique to identify different structures present in biomineralized magnetic systems. This technique encompasses enough sensitivity to probe inorganic precursors (Berger et al. 1998), as well as biomineralized magnetic material; in addition, the EPR spectra of nanometric magnetic structures depend on their size and shape. EPR was used to show the presence of magnetic material in fire ants of *Solenopsis* spp., possibly related to magnetite (Esquivel et al. 1999), and to analyse magnetic iron oxides in the abdomens of *Pachycondyla marginata* ants (Wajnberg et al. 2000) and in the abdomens of a honeybee (Takagi 1995). This report is focused on the structural and magnetic parameters of the nanoparticles in the abdomens of the honeybee *Apis mellifera* obtained from the temperature dependence of the EPR spectra.

The present results contribute to the elaboration and refinement of models on the transduction of the magnetic information in *Apis mellifera*, since biogenic magnetite is very specific for each species.

Materials and methods

As a natural process, dead bees are found at the entrance of the hive. These dead honeybees, *Apis mellifera*, were collected in São Paulo University apiary in the south of Brazil. To protect from deterioration, the honeybees were dried for 10 h at 35 °C and for 21 h at 39 °C and kept in a desiccator for future sample preparation.

The bees were extensively washed with 80% (v/v) ethanol solution to remove particles on the fur. Magnetic particle contamination was avoided using stainless steel and plastic tools. Sample D described below was used as a control.

The abdomens of honeybees were separated and macerated for EPR experiments. Samples were transferred to EPR quartz tubes and sealed under nitrogen flux to prevent oxygen contributions to the EPR signal at low temperatures. Lyophilized samples were obtained with a Labonco 75200 lyophilizer after maceration to investigate the dehydration effect. Eight macerated abdomens were used for sample A. Sample B consisted of ten lyophilized abdomens and, one week later, sample C was obtained by exposing sample B to air for two days, being fluxed with N_2 before measurement. A control sample (D) was prepared by roughly separating the second segments of the abdomens. Four EPR temperature-dependence experiments were performed: samples A and C, from 3 to 280 K, sample B from 3 to 170 K, and sample D from 5 to 200 K. Sample B spectra were very similar to sample C and are not shown.

Measurements were performed with a commercial X-band EPR spectrometer (Bruker ESP300E) operating at a microwave power of 4 mW, which is low enough not to saturate any of the lines of the spectra at low temperatures, with a 100 kHz modulation field of about 2 Oe (2 A m^{-1}) in amplitude. A helium flux cryostat (Air Products LTD-3-110) was used to control the temperature with an Au-Fe × Chromel thermocouple just below the sample.

Spectra were simulated by summing Gaussian and Lorenztian derivative lines as discussed later. The best fittings were chosen by visual inspection.

Results and discussion

Figures 1 and 2 show EPR spectra as a function of temperature for samples A and C, respectively. The spectra obtained are a complex superposition of lines whose composition can vary from one experiment to another. This can be due to the variation of the individual iron contents and/or to sample manipulation and/or to the previous sample histories, as shown by the difference between the spectra of sample A at 280 K before and after cooling (Fig. 1a).

In the low-field region a signal at $g = 4.3$, assigned to the presence of the Fe^{3+} ion, can be observed in all spectra. The intensity of this signal strongly decreases with increasing temperatures and it is easily identified in Figs. 1a and 2a.

A six-line structure is noticed in all spectra superimposed on a line at $g = 2.01$. Arrows (Mn) in Figs. 1a and 2a indicate the peak positions of this component. This signal can be identified with that obtained for the second segment of the abdomen (experimental spectrum in Fig. 1b). The envelope in $g = 2.01$ is from here on called the background line (envelope spectrum in Fig. 1b). The resonant field and linewidth of this line are temperature independent. A similar EPR signal was observed for marine particles in surface seawater from the English Channel. X-ray diffraction, EPR, Mössbauer spectroscopy, and mass susceptibility measurements of heat-treated particles support the assignment of this EPR signal to the amorphous hydroxide FeOOH (Boughriet et al. 1995). After thermal treatment of the second segments for 20 min at 350 °C followed by 20 min at 450 °C, they were examined (heated spectrum in Fig. 1b). The difference between the spectra of heated and non-heated samples (difference spectrum in Fig. 1b) reveals a relative decrease of the background line and the appearance of a broad line, indicating the conversion of FeOOH to magnetite, maghemite, or hematite. A sharp increase of the narrow $g = 2$ line is also observed. This line was truncated to have a better resolution of the other components. Furthermore, Takagi (1995) has observed one broad EPR line in only one abdomen of an

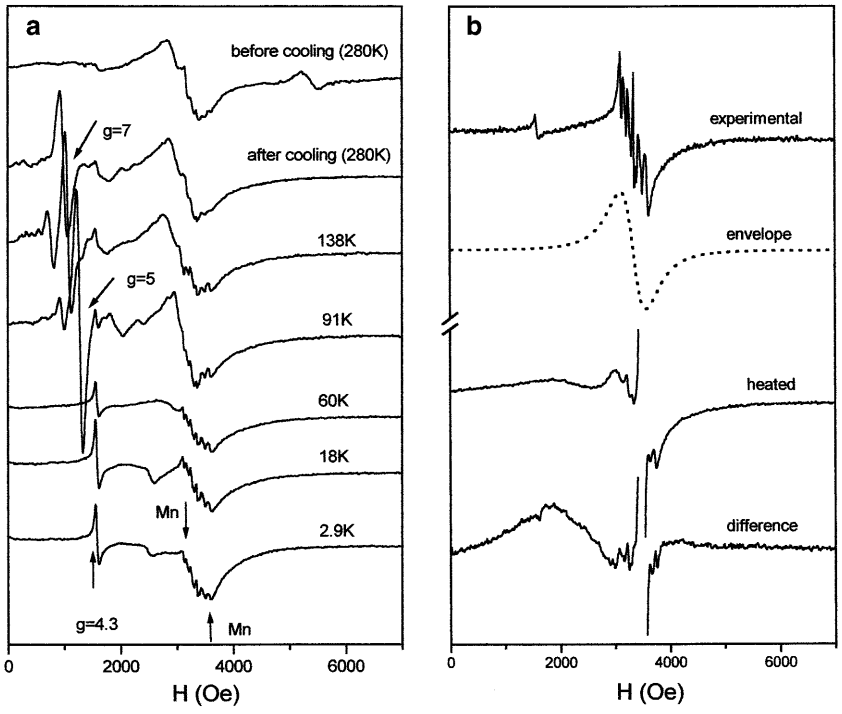

Fig. 1 Typical X-band resonances: **a** spectra of honeybee *Apis mellifera* abdomens at different temperatures for macerated sample A; **b** spectra of a second segment of abdomen at $T = 99$ K (experimental), its simulation (envelope), heat treated for 20 min at 350 °C followed by 20 min at 450 °C measured at room temperature (heated), and the difference between the spectra of heated and non-heated samples (difference)

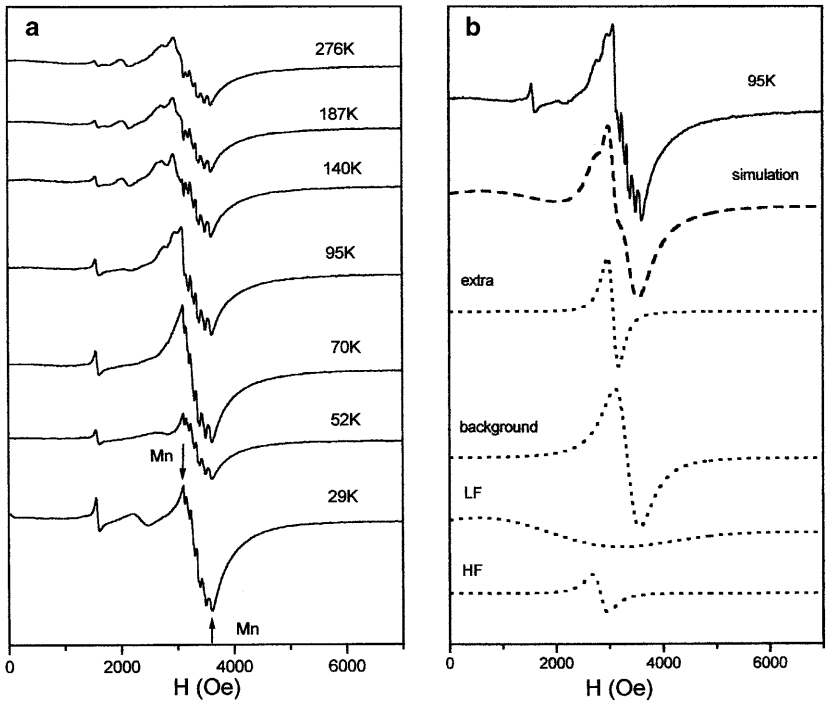

Fig. 2 **a** Typical X-band resonance spectra of honeybee *Apis mellifera* abdomens at different temperatures for the lyophilized sample C; **b** the *dashed curve* is the simulation of the spectrum at 95 K using a Gaussian component for the LF line and Lorentzian components for HF, background, and extra lines (*dotted curves*)

adult worker honeybee drastically dried, which could be compared to the background component. The failure to observe magnetic components can be related to the difference in material content from one adult individual to another, to the local origin of the bees, to the development adult stage, and to the drying treatment. The six-line feature is from manganese, which is commonly found in biological tissues. It has already been observed in the EPR spectra of ants (Krebs and Benson 1965; Esquivel et al. 1999). The high intensity of Mn and background lines relative to the isolated nanoparticles in honeybees seem to indicate higher contents of Mn and iron hydroxide particles in comparison with those found for migratory ants (Wajnberg et al. 2000).

At low temperatures the spectra show a shoulder in the $g = 2$ region observed at the low-field tail of the manganese envelope. This feature indicates the presence of another component, named the high-field (HF)

resonance line. Simulation of the spectra indeed requires a second line in this region, as shown in Fig. 2b. A very broad magnetic resonance structure is identified at high g values by its effect on the low-field baseline with a non-zero value, named the low-field (LF) resonance line (see Figs. 1a and 2a).

At temperatures higher than 60 K, sample A spectra exhibit a resonance structure at the LF region with g values between 5 and 7 (arrows in Fig. 1a) and a linewidth of about 130 Oe, named the iron line (Fe). At temperatures higher than 70 K, samples B and C exhibit a signal at $g = 2.16$ (called the extra line) that remains almost temperature independent within the visual criteria used in the simulation (Fig. 2b). Other less intense signals appear in narrow ranges of temperatures and are not discussed here.

The spectra of samples A, B, and C were simulated with a sum of Gaussian- and Lorentzian-shaped curves to obtain the temperature dependence of the resonance fields and linewidths. We noted that the LF resonance line is better simulated by a Gaussian curve, while for others lines, Lorentzian curves gave good results. The Fe line was not taken into account in the simulations and only the background Mn envelope was simulated (Fig. 1b). At temperatures lower than 25 K the background line is asymmetric and neither a Lorenztian nor a Gaussian line shape resulted in good fittings. Spectra were then simulated for temperatures higher than about 30 K.

An example of simulation is shown in Fig. 2b for the modified lyophilized sample C at 95 K. The dashed line is the sum of the HF, LF, background, and extra components (dotted lines). The background line simulation is shown as the envelope spectrum in Fig. 1b.

It is known from magnetic resonance experiments that a broad line in the $g = 2$ region is due to isolated magnetic nanoparticles, while the aggregation of these particles shifts the line to the LF region (Sharma and Waldner 1977; Fanin et al. 1993; Dormann et al. 1997). Supported by these observations, it was assumed that honeybee abdomens present two distinct magnetite-based structures: isolated nanoparticles related to the HF line and aggregates of nanoparticles related to the LF line. The characteristic signal of inorganic bulk magnetite (Ikeya 1993) was not observed in the abdomen spectra. Figures 3 and 4 show the resonance linewidth (ΔH_R) and the resonance field (H_R) associated with the HF, LF, and Fe resonance lines as a function of temperature. The anomalous results obtained for the resonance linewidths (Fig. 3) demonstrate how complex is the magnetic system. It is interesting to note the similarity of the three upper curves with the natural sample A values changing in a narrower temperature range than the B and C ones, even though the nonexistence of models to explain this behaviour. For the HF lines, ΔH_R decreases with increasing temperatures, suggesting that at low temperatures the nanoparticle moments are frozen at different orientations but at higher temperatures fluctuations are thermally activated, causing motional

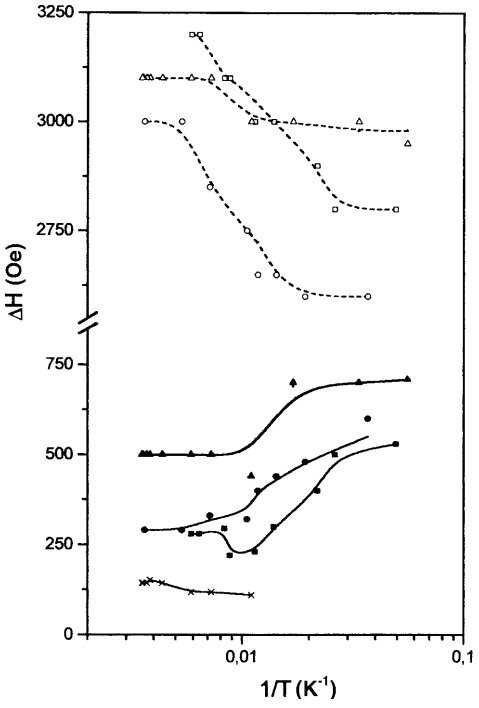

Fig. 3 Temperature dependence of the resonance linewidths of HF, LF, and Fe resonance lines. *Filled symbols* are for HF line and *open symbols* for the LF one. *Solid* (HF) and *dashed* (LF) lines are guides to the eyes. × Fe line, ▲ sample A, ■ sample B, and ● sample C

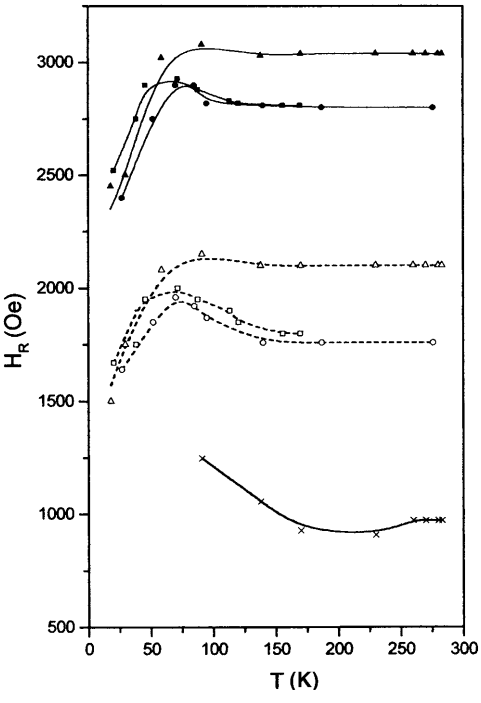

Fig. 4 Temperature dependence of the resonance field of HF, LF, and Fe resonance lines. Note that the HF and LF curves are almost parallel to each other, with the field shifted by an average value about 946 ± 66 Oe. The symbols are the same as in Fig. 3

narrowing of the resonance line. The ΔH_R of the LF and HF temperature-dependent resonance lines can be considered similar to those obtained for the migratory ant *Pachycondyla marginata* (Wajnberg et al. 2000) if different temperature ranges are compared. The increase of ΔH_R for the HF line in migratory ants from 300 to 70 K appears from 120 to 30 K in honeybees. The decrease of ΔH_R obtained for ants at temperatures lower than 70 K cannot be observed for bee abdomens, possibly because this observation could require temperatures lower than those considered. In the same way, the decrease of the ΔH_R of the LF resonance line for ants from 300 to 50 K appears from 300 to 30 K for honeybees, with the same low-temperature restriction. The ΔH_R shift suggests a lower blocking temperature, or lower magnetocrystalline energy of the nanoparticles found in bees when compared to that of migratory ants. Considering the isolated nanoparticles dispersed in a non-magnetic matrix, the linewidth approximately follows a tanh function (Morais et al. 1987). The magnetic anisotropy energy KV can then be roughly estimated from the data in Fig. 3 as $\sim 2 \times 10^{-14}$ erg and $\sim 1 \times 10^{-14}$ erg ($\sim 2 \times 10^{-21}$ J and $\sim 1 \times 10^{-21}$ J) for samples A and B, respectively. Using the K values at 280 K (given in Fig. 5, as explained below), volumes of $\sim 1 \times 10^3$ nm^3 and $\sim 3 \times 10^2$ nm^3 for samples A and B are found, respectively.

It is observed that the H_R of the HF and LF resonance lines are almost parallel in the whole temperature range (Fig. 4). This parallelism was also observed for abdomens of migratory ants and it indicates a correlation between the single-particle and the aggregated magnetic structures. However, similar to the ΔH_R results, the increase of H_R observed from about 20 K to 90 K for bees appears from 30 K to 300 K for ants. The same considerations as in Wajnberg et al. (2000) were used, where an effective field H_{EFF} is given by:

$$H_{EFF} = \omega_R/\gamma \tag{1}$$

where ω_R is the Larmor precession frequency and γ the gyromagnetic ratio. The effective field is composed of the sum of three components: the external field H_E, the demagnetizing field H_D, and the anisotropy field H_A. The external field is identified with H_R at the resonance condition. If the single-particle structure is considered as composed of spherical particles, the resonance field is given by:

$$H_R = \omega_R/\gamma - H_A \tag{2}$$

The cluster structures can be described by an ellipsoid uniformly magnetized, composed of several single particles, with a demagnetizing field H_D. The H_D field is written in terms of the demagnetizing perpendicular ($N_\perp$) and parallel ($N_{||}$) tensor components as $H_D = (N_\perp - N_{||})M_S$, where M_S is the saturation magnetization associated with the magnetic nanoparticles. If the parallel axis corresponds to the easy magnetic axis of the particle, the resonance field can be written as follows (Vonsovskii 1966; Kittel 1996):

$$H_R = \omega_R/\gamma - (N_\perp - N_{||})M_S - H_A \tag{3}$$

where $(N_\perp - N_{||}) > 0$. It is evident from Eqs. 2 and 3 that the temperature dependence of the resonance fields of both structures are determined by the anisotropy field behaviour, which should give rise to parallel curves shifted by $(N_\perp - N_{||})M_S$. An average shift of 946 ± 66 Oe between the two H_R versus T curves of the three samples A, B, and C (Fig. 4) was obtained. From this shift in the field it is possible to estimate the aspect ratio q for the ellipsoid. The two most useful ellipsoidal shapes are prolate and oblate spheroids, characterized by the three principal axes (a, b, and c), respectively elongated or flattened along the c axis, such as $c \gg a = b$ for prolate and $c \ll a = b$ for oblate. Since q is the ratio of longest to shortest axis, the demagnetizing factor for the long axis of a prolate spheroid is:

$$N_{||} = N_c = 4\pi\{q \ln[q + (q^2-1)^{1/2}]/(q^2-1)^{1/2} - 1\}/(q^2-1) \tag{4}$$

and for an oblate spheroid is:

$$N_{||} = N_a = N_b = (\pi/2)\{[q^2/(q^2-1)^{3/2}] \arcsin[(q^2-1)^{1/2}/q] - 1/(q^2-1)\} \tag{5}$$

$N_\perp$ was calculated from the relation $N_{||} + 2N_\perp = 4\pi$. The calculated field shift of 946 Oe matches $q = 1.54$

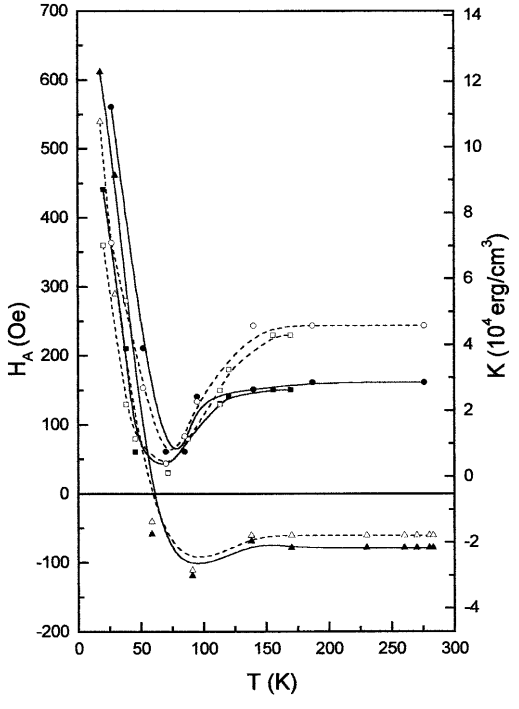

Fig. 5 Anisotropy field and anisotropy constant calculated from the resonant field values using Eqs. 2 and 3 for the HF and LF lines, respectively. The symbols are the same as in Fig. 3

or $q = 2.14$ if the system is described by a prolate or oblate ellipsoid, respectively, with the same values of $N_{||} = 2.853$ and $N_{\perp} = 4.856$. If a linear chain is considered as the cluster structure, a prolate spheroid should be assumed with $a = b$ equal to the average value of the nanoparticles' diameter. The longer axis c is then the number of particles in the chain times this diameter, so that $q = c/a$ is an integer. The q value obtained for the prolate case suggests that the structure is not a linear chain, but an agglomerate of single nanoparticles, as, for example, the stacking of two chains with three particles in each. On the other hand, if a disk or ring is considered, an oblate spheroid with $q \approx 2$ indicates an aggregate of four single particles.

Assuming the saturation magnetization value of bulk magnetite to be 471 Oe and using Eqs. 2 and 3 for the resonance field, with the parameters $\nu = 9.425 \times 10^9$ Hz and $\gamma = 2 \times 10^7\ s^{-1}\ Oe^{-1}$ (which corresponds to $g = 2.27$ for magnetite) (Raikher and Stepanov 1992), the anisotropy field H_A is obtained and shown in Fig. 5. The anisotropy field of magnetite nanoparticles is due to the effective magnetocrystalline anisotropy density (K_{EFF}) and is given by $H_A = 2K_{EFF}/M_S$. In general, K_{EFF} and M_S are both temperature dependent. However, considering that our data were taken in a temperature range far below the Curie temperature for bulk magnetite (850 K), M_S can be considered constant. Therefore, the temperature dependence derives from K_{EFF}. Figure 5 shows that above about 40 K the anisotropy field of samples B and C is higher than that of the non-lyophilized sample A. This effect can be explained considering the possibility that during the lyophilization process an oxide shell around the magnetite nanoparticles is generated. This oxide shell contributes to the anisotropy with a surface component that increases the value of effective anisotropy K_{EFF} (Gangopadhyay et al. 1992; Kodama et al. 1996; Martínez et al. 1998), as well as increasing the anisotropy field value. Based on this hypothesis, the presence of the Fe line in the non-lyophilized sample A could be explained as follows. This line is probably reflecting the presence of the magnetic material, as its resonant field temperature-dependent curve is also parallel to those of HF and LF. This signal should be related to free iron particles that are close enough to the ferromagnetic nanoparticles to be influenced by an effective magnetic field which depends on the temperature due to the effects of thermal averaging of the anisotropy field. Those free iron particles could be precursors of the magnetic particles or single ions remaining in the surrounding region of the particles. In samples B and C this signal is not present, but the extra signal appears around $g = 2$ at the same temperature range, $T > 60$ K (Fig. 2). This effect can be related to the transfer of these free iron particles by the lyophilization process to generate the oxide shells, which exhibit a resonance signal around the $g = 2$ region. A similar effect, the migration of the Fe^{3+} signal ($g = 4.3$) to the $g = 2$ region in annealed iron-containing borate glass, was already observed by Berger et al. (1998). This narrow signal, prevailing at high temperatures, was also quoted in experiments on non-interacting maghemite (γ-Fe_2O_3) nanoparticles in ferrofluids (Gazeau et al. 1999) and in studies of magnesioferrite particles (Dubowick and Baszynski 1986).

The anisotropy constant of the non-lyophilized abdomens shows a change in its sign at ~60 K. According to Belov (1993), the temperature of 130–135 K at which inorganic magnetite presents a change in sign is that of the "magnetorientation-type transition". This temperature range is close to that of the phase transition (100–120 K), known as the Verwey transition, of the induced type where electrical conductivity and other magnetic features show sharp changes. These transition temperatures depend on the presence of impurities (Syono and Ishikawa 1963; Brabers et al. 1980, 1998). The line shape and intensity changes of the EPR spectra visually evidence a transition from 60 K to 91 K for sample A and from 52 K to 72 K for samples B and C. The same is not observed in the background line of the second segment, which presents a smooth intensity decrease with increasing temperature (data not shown). A change in the EPR parameters of migratory ant abdomens is also observed at about 70 K (Wajnberg et al. 2000). These changes indicate a transition in the magnetic system, which we suggest to be related to the Verwey transition that would be shifted to lower temperatures in biogenic magnetite. In this case, the magnetite in honeybee abdomens should contain minute quantities of impurities, as shown by the quantitative analysis of the stoichiometric composition of biomineralized magnetite in bacteria (Towe and Moench 1981). Bee magnetic materials have not yet been studied in detail for impurity analysis, so this hypothesis stimulates such a study. The difference observed in the magnetic anisotropy of samples B and C relative to sample A, which differ in their degree of hydration, suggests that this structural change may be functionally important, as in other biological systems (Alberts et al. 1983).

The magnetic volume of the isolated nanoparticles estimated here corresponds to a diameter of 12 nm, in agreement with those observed by Schiff (1991), in the range from 10 to 20 nm. However, the latter nanoparticles were not identified as magnetite. Schiff and Canal (1993) developed a model for the honeybee magnetoreception, based on the observation of small nanoparticles in the base and in the lateral wall of sensorial hairs in the second abdominal ganglion (Schiff 1991). Experimental results do not allow distinguishing between the prolate and oblate geometries; nevertheless, the arrangement proposed for the agglomerate in the hair base can be interpreted as an oblate spheroid. Based on their diagram, the q value would be about 2.75, comparable to 2.14 determined in this paper. These results could partially validate the Schiff and Canal (1993) model for the honeybee magnetoreceptor organization.

Despite the large number of experiments with the honeybee *Apis mellifera*, the precise location of magnetoreceptors is still controversial (Vácha 1997). The Schiff (1991) and Hsu and Li (1994) observations of possible

magnetoreceptor locations were not reproduced. EPR results confirm the presence of magnetic nanoparticles in their abdomens. In spite of the complexity of the spectra, they were conclusively analysed based on the deconvolution of the spectral components and on the interpretation previously proposed (Wajnberg et al. 2000). The volumes of the isolated particles could only be roughly estimated, but the presence of the Fe and extra components, not observed in migratory ants experiments, enrich the discussion and stimulate proposals for the biogenic magnetite process. At least four iron structures were identified: isolated Fe^{3+} ions, FeOOH, isolated nanoparticles, and aggregates of these particles. The biomineralization process of magnetite in honeybee abdomens is still unknown. Particularly interesting is the observation of the FeOOH spectrum, since this compound was proposed to be in the pathway for magnetite biomineralization (Mann 1985).

Natural magnetites inevitably contain impurities. Titanium substitution in magnetite produces systematic variations in magnetic and physical properties, for example the magnetization of saturation, Curie temperature, coercivity, magnetocrystalline anisotropy constant, and cell parameter (Banerjee and Moskowitz 1985). The anisotropy field calculated and the observed transition of the biogenic magnetite in bee and migratory ant abdomens are distinct from that of the inorganic one. As for now, all purposed magnetoreception mechanisms must be considered in view of the difficulties of testing the magnetic navigation hypothesis even in the laboratory (Walker and Diebel 2000). Our results present new opportunities for the study of magnetite produced by organisms and are relevant to the development and validation of the models based on magnetite receptors for honeybees.

Acknowledgements We are thankful to Dr. B. Pamplona for kindly providing honeybees and D. Guenzburg for carefully reading the manuscript. M.P.L. thanks FAPERJ, E.W. thanks CNPq, and D.A.-A. thanks CLAF-CNPq for financial support.

References

Alberts B, Bray D, Lewis J, Raff M, Roberts K, Watson JD (1983) Molecular biology of the cell. Garland, New York

Banerjee SK, Moskowitz BM (1985) Ferrimagnetic properties of magnetite. In: Kirschvink JL, Jones DS, MacFadden BJ (eds) Magnetite biomineralization and magnetoreception in organisms: a new biomagnetism. Plenum Press, New York, pp 17–42

Belov KP (1993) Electronic processes in magnetite (or "enigmas of magnetite"). Phys Usp 36: 380–391

Berger R, Kliava J, Bissey JC, Baietto V (1998) Superparamagnetic resonance of annealed iron-containing borate glass. J Phys Condens Matter 10: 8559–8572

Blakemore R (1975) Magnetotactic bacteria. Science 190: 377–379

Boughriet A, Cordier C, Derane L, Ouddane B, Chamley H, Warlel M (1995) Coprecipitation/accumulation/distribution of manganese and iron, and electrochemical characteristics of Mn in calcareous seawater. Fresenius J Anal Chem 352: 341–353

Brabers VAM, Merceron T, Porte M, Krishnan R (1980) Magnetic anisotropy of magnesium ferrous ferrites. J Magn Magn Mater 15–18: 545–546

Brabers VAM, Walz F, Kronmüller H (1998) Impurity effects upon the Verwey transition in magnetite. Phys Rev B 58: 14163–14166

Diebel CE, Proksch R, Green CR, Neilson P, Walker MM (2000) Magnetite defines a vertebrate magnetoreceptor. Nature 406: 299–302

Deutschlander ME, Phillips JB, Borland SC (1999) The case for light-dependent magnetic orientation in animals. J Exp Biol 202: 891–908

Dormann JL, Fiorani D, Tronc E (1997) Magnetic relaxation in fine-particle systems. Adv Chem Phys 98: 283–494

Dubowick J, Baszynski J (1986) FMR study of coherent fine magnesioferrite particles in MgO-line shape behavior. J Magn Magn Mater 59: 161–168

Edmons DT (1992) A magnetite null detector as the migrating bird's compass. Proc R Soc (Lond) Ser B 249: 27–31

Esquivel DMS, Acosta-Avalos D, El-Jaick LJ, Cunha ADM, Malheiros G, Wajnberg E, Linhares MP (1999) Evidence for magnetic material in the fire ant *Solenopsis* sp. by electron paramagnetic resonance measurements. Naturwissenschaften 86: 30–32

Fanin PC, Scaife BKP, Charles SW (1993) Relaxation and resonance in ferrofluids. J Magn Magn Mater 122: 159–163

Gangopadhyay S, Hadjipanayis GC, Dale B, Sorensen CM, Klabunde KJ, Papaefthymiou V, Kostikas A (1992) Magnetic properties of ultrafine iron particles. Phys Rev B 45: 9778–9787

Gazeau F, Shilov V, Bacri JC, Dubois E, Gendron F, Perzynski R, Raikher YL, Stepanov VI (1999) Magnetic resonance of nanoparticles in a ferrofluid: evidence of thermofluctuational effects. J Magn Magn Mater 202: 535–546

Gould JL (1982) Ethology: the mechanisms and evolution of behavior. Norton, New York, pp 191–207

Gould JL (1985) Are animal maps magnetic? In: Kirschvink JL, Jones DS, MacFadden BJ (eds) Magnetite biomineralization and magnetoreception in organisms: a new biomagnetism. Plenum Press, New York, pp 257–268

Gould JL, Kirschvink JL, Deffeyes KS (1978) Bees have magnetic remanence. Science 201: 1026–1028

Gould JL, Kirschvink JL, Deffeyes KS, Brines ML (1980) Orientation of demagnetized bees. J Exp Biol 80: 1–8

Grissom CB (1995) Magnetic field effects in biology: a survey of possible mechanisms with emphasis on radical-pair recombination. Chem Rev 95: 3–24

Hsu CY, Li CW (1994) Magnetoreception in honeybees. Science 265: 95–97

Ikeya M (1993) Silica and silicates: geotherm and volcanism. In: Zimmerman MR, Whitehead N (eds) New applications of electron spin resonance dating, dosimetry and microscopy. World Scientific, Singapore, pp 315–353

Kirschvink JL (1989) Magnetite biomineralization and geomagnetic sensitivity in higher animals: an update and recommendations for future study. Bioelectromagnetics 10: 239–259

Kirschvink JL, Walker MM (1985) Particle-size considerations for magnetite-based magnetoreceptors. In: Kirschvink JL, Jones DS, MacFadden BJ (eds) Magnetite biomineralization and magnetoreception in organisms: a new biomagnetism. Plenum Press, New York, pp 243–256

Kirschvink JL, Jones DS, MacFadden BJ (eds) (1985) Magnetite biomineralization and magnetoreception in organisms: a new biomagnetism. Plenum Press, New York

Kirschvink JL, Kobayashi-Kirschvink A, Woodford BJ (1992) Magnetite biomineralization in the human brain. Proc Natl Acad Sci USA 89: 7683–7687

Kirschvink JL, Diaz-Ricci JC, Nesson MH, Kirschvink SJ (1993) Magnetite-based magnetoreceptors in animals: structural, behavioral and biophysical studies. Technical Report TR-102008, Electric Power Research Institute, Palo Alto, Calif

Kittel C (1996) Introduction to solid state physics. Wiley, New York

Kodama RH, Berkowitz AE, McNiff EJ, Foner S (1996) Surface spin disorder in $NiFe_2O_4$ nanoparticles. Phys Rev Lett 77: 394–397

Krebs AT, Benson BW (1965) Electron spin resonance in Formicidae. Nature 207: 1410–1413

Leask MJ (1977) A physicochemical mechanism for magnetic field detection by migratory birds and homing pigeons. Nature 267: 144–145

Lohmann KJ, Johnsen S (2000) The neurobiology of magnetoreception in vertebrate animals. Trends Neurosci 23: 153–159

Lowenstam HA (1981) Minerals formed by organisms. Science 211: 1126–1131

Mann S (1985) Structure, morphology, and crystal growth of bacterial magnetite. In: Kirschvink JL, Jones DS, MacFadden BJ (eds) Magnetite biomineralization and magnetoreception in organisms: a new biomagnetism. Plenum Press, New York, pp 311–332

Martínez B, Roig A, Molins E, González-Carreño T, Serna CJ (1998) Magnetic characterization of γ-Fe_2O_3 nanoparticles fabricated by aerosol pyrolysis. J Appl Phys 83: 3256–3262

Morais PC, Lara MCFL, Skeff Neto K (1987) Electron paramagnetic resonance in superparamagnetic particles dispersed in a non-magnetic matrix. Phil Mag Lett 55: 181–183

Presti DE (1985) Avian navigation, geomagnetic field sensitivity and biogenic magnetite. In: Kirschvink JL, Jones DS, MacFadden BJ (eds) Magnetite biomineralization and magnetoreception in organisms: a new biomagnetism. Plenum Press, New York, pp 455–482

Raikher YL, Stepanov VI (1992) The effect of thermal fluctuations on the FMR line shape in dispersed ferromagnets. Sov Phys JETP 75: 764–771

Rosenblum B, Jungerman RL, Longfellow L (1985) Limits to induction-based magnetoreception. In Kirschvink JL, Jones DS, MacFadden BJ (eds) Magnetite biomineralization and magnetoreception in organisms: a new biomagnetism. Plenum Press, New York, pp 223–232

Sakaki Y and Motomiya T (1990) Possible mechanism of biomagnetic sense organ extracted from sockeye salmon. IEEE Trans Mag 26: 1554–1556

Schiff H (1991) Modulation of spike frequencies by varying the ambient magnetic field and magnetite candidates in bees (*Apis mellifera*). Comp Biochem Physiol A 100: 975–985

Schiff H, Canal G (1993) The magnetic and electric fields induced by superparamagnetic magnetite in honeybees. Biol Cybern 69: 7–17

Schmidt-Koenig K, Keeton WT (1978) Animal migration, navigation and homing. Springer, Berlin Heidelberg New York

Schultheiss-Grassi PP, Wessiken R, Dobson J (1999) TEM investigations of biogenic magnetite extracted from the human hippocampus. Biochem Biophys Acta 1426: 212–216

Sharma VK, Waldner F (1977) Superparamagnetic and ferrimagnetic resonance of ultrafine Fe_3O_4 particles in ferrofluids. J Appl Phys 48: 4298–4302

Shcherbakov VP, Winklhofer M (1999) The osmotic magnetometer: a new model for magnetite-based magnetoreceptors in animals. Eur Biophys J 28: 380–392

Syono Y, Ishikawa Y (1963) Magnetocrystalline anisotropy of $xFe_2TiO_4(1–x)Fe_3O_4$. J Phys Soc Jpn 18: 1230–1231

Takagi S (1995) Paramagnetism in honeybees. J Phys Soc Jpn 64: 4378–4381

Towe KM, Moench TT (1981) Electron-optical characterization of bacterial magnetite. Earth Planet Sci Lett 52: 213–220

Vácha M (1997) Magnetic orientation in insects. Biol Bratislava 52: 629–636

Vonsovskii SV (1966) Ferromagnetic resonance. Pergamon Press, New York

Wajnberg E, Acosta-Avalos D, El-Jaick LJ, Abraçado L, Coelho JLA, Bakuzis AF, Morais PC, Esquivel DMS (2000) EPR study of migratory ant *Pachycondyla marginata* abdomens. Biophys J 78: 1018–1023

Walker MM, Diebel CE (2000) Structure, function and use of the magnetic sense in animals. J Appl Phys 87: 4653–4659

Wiltschko R, Wiltschko W (1995) Magnetic orientation in animals. Springer, Berlin Heidelberg New York

Yorke ED (1985) Energetics and sensitivity considerations of ferromagnetic magnetoreceptors. In: Kirschvink JL, Jones DS, MacFadden BJ (eds) Magnetite biomineralization and magnetoreception in organisms: a new biomagnetism. Plenum Press, New York, pp 233–242